

ORIGINAL RESEARCH

IL-27-induced, MSC-derived Exosomes Promote MMP3 Expression Through the miR-206/L3MBTL4 Axis in Synovial Fibroblasts

Lihui Ma, MD; Yueli Liu, MMed; Fenghuang Xu, MMed; Ruiming Shen, MMed; Min Wang, MMed; Yunfei Zhang, MMed; Chang Liu, MMed; Guifu Zheng, MMed;

ABSTRACT

Context • In rheumatoid arthritis (RA), hyperproliferative fibroblast-like synoviocytes (FLS) can secrete a variety of tissue hydrolases, such as matrix metalloproteinases (MMPs), causing the destruction of chondrocytes. Mesenchymal stem cells (MSCs) can directly affect FLS through extracellular vesicles (EVs). Interleukin-27 (IL-27) is a pleiotropic immune regulator frequently overexpressed in RA.

Objective • The study intended to examine the effects of IL-27-induced exosomes from bone-marrow mesenchymal stem cells (BM-MSCs) and to determine if they promote the secretion of MMP3 in synovial cells.

Design • The research team performed a genetic study.

Setting • The study took place at the First Affiliated Hospital of Hainan Medical University in Haikou City, Hainan, China.

Outcome Measures • The research team: (1) determined if IL-27 expression had occurred in the synovial fluid; (2) co-cultured IL-27-induced MSCs with FLS to detect the expression of MMP3 in the FLS; (3) Under IL-27 induction, MSC-derived exosomes with IL-27R knockdown were collected to detect the expression of microRNAs(miRNAs) associated with RA; (4) screened the miRNAs to determine

the most significant differences in expression; (5) determined the miRNA target genes in arthritis, using Western blot (WB) and qRT-PCR; and (6) Dual luciferase and ChIP experiments confirm regulation of MMP3 by L3MBTL4.

Results • IL-27 was highly expressed in RA, and the IL-27-induced, MSC-derived exosomes promoted the expression of MMP3 in FLS. The IL-27-induced MSC-derived exosomes significantly upregulated the expression of miR-206-3p, and the miR-206-3p target, miR-206/lethal(3) malignant brain tumor-like protein 4 (L3MBTL4), regulated the MMP3 transcription. The IL-27-induced, MSC-derived exosomes promoted MMP3 expression in the FLS through the miR-206-3p/L3MBTL4 axis, thereby promoting chondrocyte degradation and aggravating RA.

Conclusions • IL-27 can induce the expression of miR-206 in MSCs, and miR-206 can be transported into FLS through MSC-EVs to promote FLS migration and MMP3 expression and aggravate articular cartilage damage. Patients with RA who have a high IL-27 expression may not be suitable to receive treatment with MSCs, and clinicians can use MSCs that knock down or delete IL-27R to treat RA patients who have a high IL-27 expression. (*Altern Ther Health Med.* 2023;29(8):680-688).

Lihui Ma, MD; Fenghuang Xu, MMed; Ruiming Shen, MMed; Min Wang, MMed; Chang Liu, MMed; Guifu Zheng, MMed; Department of Rheumatology and Immunology, the First Affiliated Hospital of Hainan Medical University, Haikou City, Hainan, China. **Yueli Liu, MMed;** Department of Pharmacology, Hainan Medical University, Haikou City, Hainan, China. **Yunfei Zhang, MMed;** Biological Science, the College of Liberal Arts and Sciences, Arizona State University, Tempe, Arizona, USA.

Corresponding author: Lihui Ma, MD

E-mail: marymlh0826@163.com

Rheumatoid arthritis (RA) is a systemic autoimmune disease in which the synovium is the central player, with RA being characterized by inflammatory synovitis.¹ The

synovium protects the joints primarily by producing a lubricant and providing cartilage that lacks its own blood supply. The synovium mainly comprises macrophage-like synovial cells, fibroblast-like synoviocytes (FLS), adipocytes, blood vessels, and scattered immune cells.²

The global incidence of RA is approximately 0.24%.³ Current drugs only alleviate RA's symptoms and don't achieve a cure. Although researchers have extensively studied the pathogenesis of RA in recent years, they haven't determined the exact process due to the complexity of RA's mechanisms.⁴⁻⁶

Pathogenic Factors

Two key pathogenic factors in the synovium contribute to exacerbation of RA. First the macrophage-like synovial cells produce a variety of pro-inflammatory cytokines that trigger an inflammatory response, and second, the FLS

proliferate, produce a large number of matrix metalloproteinases (MMPs), destroy cartilage tissue, and cause joint damage.^{6,7}

Joint destruction in RA mainly occurs in cartilage sites that pannus hyperplasia has infiltrated. Hyperproliferative FLS secrete a variety of tissue hydrolases, such as MMPs mentioned above, accelerating the degradation of cartilage extracellular matrix and causing the destruction of chondrocytes.

The proliferation of FLS can release a large amount of MMPs, which are the main cause of joint damage in RA. Among them, MMP3 is highly expressed in RA and is a biomarker of it,⁸⁻¹⁰ and RA-FLS can secrete more MMP3.¹¹

Mesenchymal Stem Cells (MSCs)

In recent years, treatment of RA using MSCs has become a new therapeutic approach. MSCs are a class of self-renewing, pluripotent stem cells widely used in tissue regeneration and damaged-cell repair.¹² Two recent studies found that MSC transplantation (MSCT) can effectively treat RA by reducing joint inflammation, bone erosion and destruction, and pannus formation through immunomodulation, anti-inflammatory effects, and differentiation.^{13,14} Spees et al and Kodama et al found that MSCs can exert regulatory effects, mainly through the release of extracellular vesicles (EVs) and paracrine cytokines.^{15,16}

Inflammatory Process

Multiple cytokines and their feedback loops subtly regulate complex immune responses and inflammatory development in RA.¹⁷ Interleukin-27 (IL-27) is a soluble cytokine, a pleiotropic immune regulator frequently overexpressed in RA.

Some studies have found elevated levels of IL-27 in the blood, synovial fluid, and rheumatoid nodules of patients with RA.¹⁸⁻²² Therefore, IL-27 may be directly or indirectly involved in RA pathogenesis.²³

Xu et al's study showed that IL-27 can regulate the proliferation and migration of MSCs.²⁴ Chen et al found that EVs derived from bone-marrow MSCs (BM-MSCs) had transferred microRNA-150-5p (miR-150-5p) to the FLS.²⁵ The miRNA secretion through MSC-EVs (MSC-EV-miRNAs) modulates multiple signaling pathways that target specific proteins, thereby affecting the development of RA.

IL-27 upregulates the expression of microRNA-206 (miR-206) in MSCs and MSC-EVs through IL-27R. MSC-EVs may transport miR-206 into FLS and inhibit the migration of FLS and the expression of MMP3. As is generally known, MSC-EVs can deliver miRNAs to the target recipient cells.

The transfer of miR-150-5p in BM-MSCs by exosomes to RA-FLS can repress the target gene MMP14.²⁵ Transfers of MSC-exosomal miR-192-5p to synovial tissue can inhibit synovial hyperplasia and joint destruction,²⁶ and MSC-EVs overexpressing miR-124a can inhibit the proliferation of arthritic FLS MH7A.²⁷ Therefore, MSC-EV's miRNAs are potential biomarkers for novel, cell-free, therapeutic strategies for RA.

Current Study

The study intended to examine the effects of IL-27-induced exosomes from BM-MSCs and to determine if they promote the secretion of MMP3 in synovial cells.

METHODS

The research team performed a genetic study, which took place at the First Affiliated Hospital of Hainan Medical University in Haikou City, Hainan, China.

Animals

8-week-old male Sprague-Dawley (SD) rats were obtained from Beijing Vital River Laboratory Animal Technology Co. Ltd. All procedures were approved by Hainan Medical University Animal Care and Use Committee. The rats were housed in polystyrene cages in a temperature-controlled room (21°C) with 55% humidity, 12-hour light/dark cycle, and standard rodent chow and water ad libitum. SD rats were divided into two groups, one control group and one CIA modeling group, 10 rats in each group.

Procedures

Materials. The research team obtained: (1) the human arthritic (RA)-FLS cell lines, MH7A and 293, from the American Type Culture Collection (ATCC) in Gaithersburg, MD, USA; (2) Roswell Park Memorial Institute-1640 (RPMI-1640) from Gibco (Grand Island, NE, USA); (3) Dulbecco's Modified Eagle Medium (DMEM) from Gibco (Grand Island, NE, USA); (4) fetal bovine serum (FBS) from Gibco (Grand Island, NE, USA); (5) small interfering RNA (siRNA) from genepharma (Shanghai, China); (6) IL-27 from medchemexpress (New Jersey, USA); (7) the psiCHECK2 vector from Synbio Technologies (Suzhou, China); (8) miR-206-3p mimic, miR-206-3p inhibitor, mimic nc, and inhibitor nc from Shbio (Shanghai, China); (9) TRIzol reagent from Invitrogen (Carlsbad, CA, USA); (10) Random Primer 6 from Thermofisher (Waltham, MA, USA); (11) A6002 qRT-PCR mix and dual-luciferase reporter assay from Promega (Madison, WI, USA); (12) CFX96 touch system from Biorad (Hercules, CA, USA); (13) gel-electrophoresis equipment from Biorad (Hercules, CA, USA); (14) polyvinylidene fluoride (PVDF) membrane and protein A/G magnetic beads from Millipore (Darmstadt, Germany); (15) anti-IL-27R, ab216347, and Lipofectamine 2000 from Invitrogen (Carlsbad CA, USA); (16) anti-MMP3, ab52915; anti-L3MBTL4, ab235089; a ChIP assay kit, ab500; an anti-enhancer of zeste homolog 2 (EZH2) antibody, ab191250; and anti-H3K27me3 antibody, ab6002; from Abcam (Cambridge, England); (17) anti-glyceraldehyde 3-phosphate dehydrogenase (GAPDH) antibody, 10494-1-AP; goat anti-rabbit, SA00001-2; and goat anti-mouse, SA00001-1, from Proteintech (Wuhan, China); (18) paraformaldehyde from sigma (Darmstadt, Germany); (19) phosphate buffered saline (PBS) from Gibco (Grand Island, NE, USA); (20) crystal violet from Beyotime (Shanghai, China); (21) Transwell plates from Corning (Corning, NY, USA); and (22) normal rabbit immunoglobulin G (IgG) from Millipore (Darmstadt, Germany).

Induction of RA. Before CIA was established, rats were anesthetized using 1% sodium pentobarbital (40 mg/kg) by intraperitoneal injection. Type II collagen was dissolved to 4 mg /mL in 0.05 mol/L acetic acid. Collagen was prepared by emulsifying an equal amount of incomplete Freund's adjuvant using an electric homogenizer. 0.1 mL of the emulsion was taken to subcutaneously inoculate CIA rats on day 0 and day 7, respectively.

Cell culture and transfection. The research team: (1) cultured the RA-FLS cells in RPMI-1640 or DMEM, with 10% FBS; (2) transfected 20 nM of siRNA, designed and synthesized 3 siRNAs, siRNA1, siRNA2, and siRNA3 respectively against IL-27R and L3MBTL4 or the control into MH7A cells; (3) achieved overexpression or inhibition of miR-206-3p through transfection with 20 nm of miR-206-3p mimic or miR-206-3p inhibitor into MH7A cells; and (4) used mimic nc or inhibitor nc as negative controls. Table 1 shows the nucleotide sequences used in these experiments.

Quantitative reverse transcription polymerase chain reaction (qRT-PCR) assay. The research team: (1) extracted the MH7A cells using TRIzol; (2) used 1 ug of RNA for reverse transcription with Random Primer 6; (3) configured the reaction system according to the manufacturer's instructions for the qRT-PCR mix; and (4) amplified the mix using the CFX96 touch system for 40 cycles. Table 2 presents the primer sequences.

Western blotting. The research team: (1) subjected 30 µg of denatured protein from MH7A cells to gel electrophoresis to separate the protein (2) transferred the protein to the PVDF membrane; (3) incubated the PVDF with protein at 4°C overnight with the primary antibodies: anti-IL-27R at 1:1000; anti-MMP3 at 1:1000; anti-L3MBTL4 at 1:500; and anti-GAPDH at 1:2000 for the protein quantification control; (4) incubated the PVDF with primary antibodies for 1 h with the secondary antibodies: goat anti-rabbit at 1:5000 or goat anti-mouse at 1:5000 at room temperature (RT).

Embedded cell co-culture. The research team: (1) transferred 5 x 10⁵ MH7A cells to the upper chamber of a Transwell plate containing serum-free culture medium and transferred 5 x 10⁵ MSC to the lower chamber containing culture medium with 5% FBS; (2) after 48 h of incubation, used 4% paraformaldehyde for 15 min to fix the cells; and (3) washed the cells with PBS and stained them with 0.1% crystal violet for 10 min. For the Transwell invasion assay, the experimental procedure was similar to that for the Transwell migration assay, using Transwell invasion plates.

Dual-luciferase assay. The research team: (1) broke the L3MBTL4 3' untranslated region (UTR) - wild type (WT) and L3MBTL4 3'UTR - mutant (MUT) sequences into the psiCHECK2 vector, using Lipofectamine; (2) constructed the psiCHECK2 luciferase-reporter plasmid with an miRNA or NC mimic and transfected into 293 cells, using Lipofectamine 2000; (3) subcloned the MMP3 promoter sequence into the pGL3 luciferase reporter vector and the pGMLR-TK luciferase reporter vector as controls; and (4) after 48 h, estimated firefly and Renilla fluorescence values using the dual-luciferase reporter assay.

Table 1. Sequence of siRNAs Targeting IL-27R and miR-206/L3MBTL4 and miR-206 Mimics and Inhibitor

Name	Sequence 5'-3'
IL-27R-siRNA-1	GCUGGAGAUUUACUACAACU
IL-27R-siRNA-2	GCAAUUCUGGGCAACCUUACA
IL-27R-siRNA-3	AGCUCAGAAUACCCUGUAACU
IL-27R-si-con	GGCTCAATCCTCGAACAGAT
L3MBTL4-siRNA-1	GGUACUUUGAAAGAACAGAAGG
L3MBTL4-siRNA-2	AGCGAACGAAUGACCCUGAAGA
L3MBTL4-siRNA-3	CAGCACUGAAGAUUUACAACU
L3MBTL4-si-con	GGAACAAGATCCGAAGAGTCA
miR-206 mimics	UGGAAUGUAAAGGAAGUGUGGG
mimics nc	UAGUAGUUAGUAAAGGGUGGAGG
miR-206 inhibitor	CCACACACUCCUUAACAUUCCA
Inhibitor nc	CUCAUCCUAAACCCUCUCAAAC

Abbreviations: IL-27R, interleukin-27R; L3MBTL4, lethal (3) malignant brain tumor-like protein 4; miR-206, microRNA-206; siRNA, short interfering RNA.

Table 2. Primer Sequences for Analysis of Expression of Various RNAs and miRNAs

Gene symbol	Forward 5'-3'	Reverse 5'-3'
MMP3	CTGGGTCTCTTCACTCAG	GAGGTCCATAGAGGGACTG
IL-27R	GTACCAAGACACAGCTCAG	GTTGGCAGAGTGGCAGTCTG
L3MBTL4	CTTCTGCTTCTGACACAG	GTTCCTGGGAATGCCTGAAC
GAPDH (human)	TGCACCACCAACTGCTTAG	CATCCACAGTCTTCTGGGTG
U6	GTGCTCGCTTCGGCAGCAC	GGAACGCTTCACGAAATTGC
miR-206	ACACTCCAGCTGGGTGGAATGTA AGGAAGTGTGTGG	CTCAACTGGTGTCTGTGGA
cel-miR-39-3p (control)	ACACTCCAGCTGGGTCAACCGGG TGTAATCAGCTTG	CTCAACTGGTGTCTGTGGA
Stem-loop universal reverse transcription primer	CTCAACTGGTGTCTGTGAGTCCGG CAATTCAGTTGAGGAAAACGC	

Abbreviations: GAPDH, glyceraldehyde-3-phosphate dehydrogenase; IL-27R, interleukin-27R; L3MBTL4, lethal (3) malignant brain tumor-like protein 4; miR-206, microRNA-206, MMP3, matrix metalloproteinase 3.

Chromatin immunoprecipitation (ChIP) assay. The research team followed the operational steps in the instructions for the ChIP kit. The team: (1) cross-linked 1 x 10⁷ FLS cells with 1% formaldehyde; (2) incubated them for 10 min at room temperature; (3) terminated the assay with 125 mM glycine; (4) lysed the cells using the ChIP lysis buffer, supplemented with a protease-inhibitor cocktail, and used chromatin fragments from 200 to 400bp; (5) used a 10% lysis mixture as input and coupled the protein A/G magnetic beads with the anti-L3MBTL4 at 1:50, with the EZH2 antibody at 1:30, with the anti-H3K27me3 antibody at 1:50, and with normal rabbit IgG as the negative control; and (6) incubated the mixtures for 4 h. The team: (1) incubated the magnetic beads of the coupled antibody with the chromatin fragments for 6 h, (2) eluted the DNA, and performed qRT-PCR in three independent replications.

Outcome Measures. The research team: (1) determined if IL-27 expression had occurred in the synovial fluid; (2) co-cultured IL-27-induced MSCs with FLS to detect the expression of MMP3 in the FLS; (3) Under IL-27 induction, MSC-derived exosomes with IL-27R knockdown were collected to detect the expression of microRNAs(miRNAs) associated with RA; (4) screened the miRNAs to determine the most significant differences in expression; (5) determined the miRNA target genes in arthritis, using Western blot (WB) and qRT-PCR; and (6) Dual luciferase and ChIP experiments confirm regulation of MMP3 by L3MBTL4.

Outcome Measures

IL-27-induced MSCs. The research team extracted MSCs from the rats and used immunofluorescence to identify positive stem-cell markers, such as cluster of differentiation 105 (CD105), CD90, and CD73, and negative stem-cell markers, such as human leukocyte antigen (HLA)-DR, CD45, and CD31. IL-27-induced MSC were co-cultured with FLS to detect the effect of IL-27-induced MSC on the invasive ability of FLS and the expression and secretion of MMP3 in the FLS.

Knockdown of IL-27R in MSCs. IL-27 mainly transmits signals into cells through the IL-27 receptor (IL-27R) on the cell membrane and regulates cells' activities.²⁸ The research team detected the knockdown efficiency of IL-27R qRT-PCR and WB screened the highest knockdown efficiencies for subsequent experiments. Knockdown of IL-27R attenuated the effect of IL-27 on MSC; therefore, MSC with knockdown of IL-27R were co-cultured with FLS, further confirming that IL-27-induced MSC can regulate the invasive ability of FLS and the expression and secretion of MMP3 in the FLS.

IL-27-induced, MSC-derived Exosomes. MSCs mainly function through paracrine extracellular vesicles. The research team extracted and identified exosomes of MSCs using electron microscopy and co-cultured the exosomes with and without IL-27-induction with FLSs. The aim was to detect IL-27-induced effects of MSC-derived exosomes on the invasive ability of FLS and the expression and secretion of MMP3 in the FLS.

miR-206. A study by de Almeida et al found that multiple miRNAs were associated with arthritis.²⁹ The research team detected the expression of miRNAs in IL-27-induced MSCs and their exosomes. Screening of IL-27-induced MSC-derived exosomes for miRNAs with critical effects on FLS migration and MMP3 expression and secretion by detecting these RA-related miRNAs.

miR-206 target L3MBTL4. To find the target of miR-206, the research team performed a target analysis of miR-206 in RA, We refer to de Almeida R et al. who analyzed the expression network of RA-associated miRNAs related targets²⁴ and identified the top 5 genes with significant expression changes by qRT-PCR. Further elucidation of the mechanisms by which exosomes regulate FLS invasiveness and MMP3 expression and secretion in FLS via miRNAs.

L3MBTL4-regulated MMP3 transcription. L3MBTL4 is a histone methyl-lysine-binding protein that is a component of the polycomb group (PcG) and maintains the transcriptionally repressed state of genes. Two main types of PcG complexes exist: polycomb repressive complex 1 (PRC1) and PRC2, and the methylation of histone H3Lys27 is the core protein EZH2 in PRC2. ChIP-qRT-PCR detection of H3Lys27 and EZH2 binding in the promoter region of MMP3 to elucidate the mechanism of MMP3 regulation by L3MBTL4 in the presence of miR-206 mimics and L3MBTL4 knockdown conditions, respectively.

Statistical Analysis

The research team analyzed all data using GraphPad Prism 8 (GraphPad, San Diego, USA). The team: (1) expressed

the data for the categorical variables and as means \pm standard deviation (SDs) and compared the groups using Student's *t* test, and for continuous variables and calculated the median and IQR, and (2) compared multiple groups using a one-way analysis of variance (ANOVA). *P* < .05 indicated a significant difference.

RESULTS

IL-27-induced MSCs

The MSCs highly expressed positive stem-cell markers—CD105, CD90 and CD73—whereas they slightly expressed negative stem-cell markers—CD31, HLA-DR and CD45 (Figure 1A).

Figure 1B shows that IL-27 was significantly higher in the synovial fluid of rats with collagen-induced arthritis than in rats without arthritis (*P* < .001). The co-culture of IL-27-induced MSCs with the FLS MH7A cells promoted FLS invasion (Figures 1C and 1D). The MSC+IL-27 group's cell count was significantly higher than that of the MSC cells (*P* < .001), which might promote pannus formation in patients with RA.

Simultaneously, IL-27-induced MSCs promoted the expression and secretion of MMP3 in FLS (Figures 1E, 1F, and 1G). The MSC+IL-27 group's mRNA expression, relative protein level, and concentration of MMP3 were significantly higher than those of the MSC cells (all *P* < .001). Higher MMP3 levels can aggravate chondrocyte destruction.

Knockdown of IL-27R in MSCs

Figures 2A and 2B show that IL-27R was knocked down in the MSCs. The siRNA1's and siRNA2's relative IL-27R mRNA expression, at *P* < .001 and *P* < .05, respectively, and relative IL-27R protein levels, at *P* < .001 and *P* < .05, respectively, were significantly lower than those of the control.

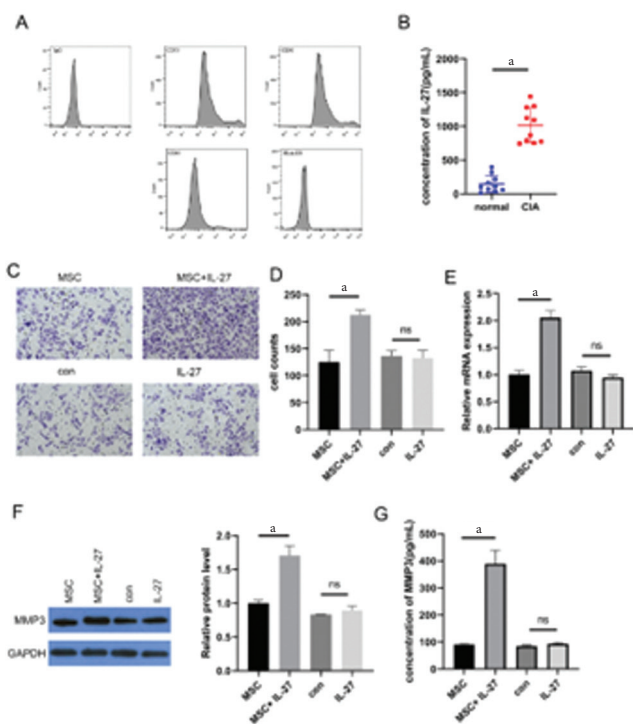
In the presence of IL-27, the MSCs knocked down for IL-27R inhibited the invasion of FLS (Figure 2C) and inhibited the expression and secretion of MMP3 in FLS (Figures 2D, 2E, and 2F). IL-27+MSC-IL-27R-1 group's cell count, relative MMP3 mRNA expression, and concentration of MMP3 were significantly lower than those of IL-27 +MSC-si-com group (all *P* < .001). Therefore, clinicians can potentially use IL-27R-knockdown MSCs to treat RA.

IL-27-induced, MSC-derived Exosomes

Figure 3A and 3B shows the exosomes of MSCs. There were four groups of exosomes in total, exosomes of MSC, exosomes of MSC induced by IL-27, exosomes of MSC induced by IL-27 containing knockdown control, and exosomes of MSC induced by IL-27 and knocking down IL-27R. The MSC-derived exosomes with IL-27 induction promoted the migration and invasion of FLS and the expression and secretion of MMP3.

The MSC exosomes with IL-27R knockdown reduced the invasion of FLS and the expression and secretion of MMP3 (3C, 3D, 3E, 3F, and 3G). The IL-27 group's cell counts were significantly higher than those of the controls. (*P* < .001), and the IL-27+si-IL-27R cells' relative MMP3

Figure 1. Promotion of Expression of MMP3 in FLS, Induced by IL-27 in BN-MSCs. Figure 1A shows the negative and positive markers of MSCs identified using flow cytometry; Figure 1B shows the expression of IL-27 in the synovial fluid of CIA-SD rats compared with the synovial fluid of normal rats; Figures 1C and 1D show the IL-27-treated MSCs co-cultured with arthritic MH7A cells, indicating the invasion ability of MH7A, detected using Transwell assays; Figure 1E shows the effect of IL-27-treated MSCs on the expression of MMP3 in MH7A cells, detected using qRT-PCR; Figure 1F shows the effect of IL-27-treated MSCs on the expression of MMP3 in MH7A cells, detected using WB; and Figure 1G shows the effect of IL-27-treated MSCs on MMP3 secretion in MH7A cells, detected using ELISA and immunofluorescence.



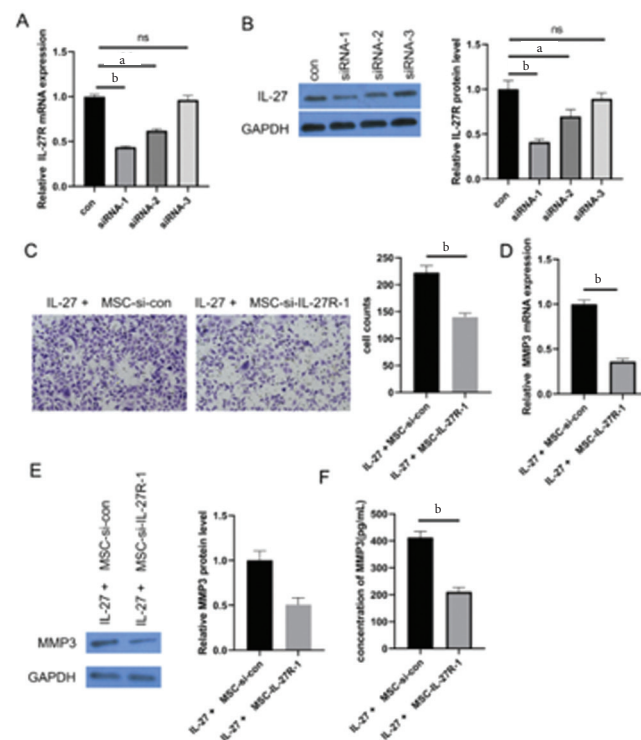
^a*P* < .001, indicating that IL-27 was significantly higher in the synovial fluid of rats with collagen-induced arthritis than in mice without arthritis (Figure 1B), that the MSC+IL-27 cells' cell count was significantly higher than that of the MSC cells (Figure 1C and 1D), and that the MSC+IL-27 cells' mRNA expression, relative protein level, and concentration of MMP3 were significantly higher than those of the MSC cells (Figure 1E, 1F, and 1D)

Abbreviations: CIA, collagen-induced arthritis; SD rats Sprague-Dawley rats; ELISA, enzyme-linked immunosorbent assay; FLS, fibroblast-like synoviocytes; IL-27, interleukin-27; MMP3, matrix metalloproteinase 3; BM-MSC, bone-marrow mesenchymal stem cell; qRT-PCR, quantitative reverse transcription-polymerase chain reaction; WB, Western blotting.

mRNA expression was significantly lower than that of the IL-27+si-con cells (*P* < .05).

The MSC-exo group's relative MMP3 mRNA expression, relative MMP3 protein level, and concentration of MMP3 were significantly lower than those of the MSC-exo (IL-27) group (all *P* < .001). The si-IL-27R-MSC-exo (IL27) group's relative MMP3 mRNA expression (*P* < .001), relative MMP3 protein level (*P* < .001), and concentration of MMP3 (*P* <

Figure 2. Alleviation of the Release by MMP3 from FLS With IL-27R Knocked Down by MSCs. Figures 2A and 2B show the efficiency of the siRNA target IL-27R, detected using RT-qPCR and WB; Figure 2C shows the effect of IL-27R knockdown MSCs on the invasion of MH7A cells in the presence of IL-27, detected using a co-cultured assay; and Figures 2D, 2E and 2F show the effect of IL-27R knockdown MSCs on the secretion of MMP3 in MH7A cells, the presence of IL-27, detected using qRT-PCR, WB, and ELISA.



^a*P* < .05, indicating that siRNA2's relative IL-27R mRNA expression and relative IL-27R protein levels were significantly lower than those of the control (Figures 2A and 2B)

^b*P* < .001, indicating that siRNA1's relative IL-27R mRNA expression and relative IL-27R protein levels were significantly lower than those of the control (Figures 2A and 2B) and that IL-27+MSC-IL-27R-1's cell count, relative MMP3 mRNA expression, and concentration of MMP3 were significantly lower than those of IL-27 +MSC-si-con (Figures 2D, 2E, and 2F)

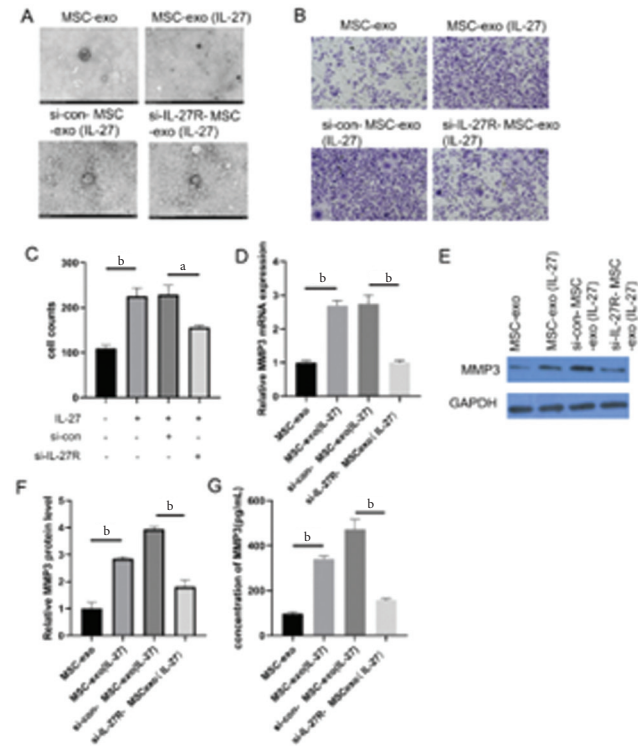
Abbreviations: ELISA, enzyme-linked immunosorbent assay; FLS, fibroblast-like synoviocytes; IL-27, interleukin-27; matrix metalloproteinase 3 (MMP3); MSC, mesenchymal stem cells; qRT-PCR, quantitative reverse transcription-polymerase chain reaction; WB, Western blot.

.001) were significantly lower than those the si-con MSC-exo (IL27) group.

miR-206 qRT-PCR detection of miRNAs associated with RA

The miR-206 had the most significant effect on IL-27-induced MSCs and their exosomes. Figure 4A shows that the BMSC group's relative miR-206 and miR-155-5P expressions were significantly higher than those of the BMSC+IL-27

Figure 3. IL-27-induced, MSC-derived Exosomes' Promotion of the Expression of MMP3 in Synovial Fibroblasts. Figure 3A shows the electron microscope identification of exosomes; Figure 3B and 3C show the IL-27-induced MSCs and IL-27R knockdown MSC exosomes, co-cultured with MH7A cells, and the invasion of MH7A cells, detected using Transwell assays; and Figure 3D, 3E, 3F, and 3G show the exosomes derived from IL-27-induced MSCs and IL-27R-knockdown MSCs, co-cultured with MH7A cells, using qRT-PCR, WB, and ELISA to detect the expression and secretion of MMP3 in MH7A cells.



^a $P < .05$, indicating that the IL-27+si-IL-27R cells' relative MMP3 mRNA expression was significantly lower than that of IL-27+si-con cells (Figure 3C)
^b $P < .001$, indicating that IL-27 group's cell counts were significantly higher than those of the controls, si-con, that the MSC-exo group's relative MMP3 mRNA expression, relative MMP3 protein level, and concentration of MMP3 were significantly lower than those of the MSC-exo (IL-27) group, and that the si-IL-27R-MSCexo (IL27) group's relative MMP3 mRNA expression, relative MMP3 protein level, and concentration of MMP3 were significantly lower than those the si-con MSC-exo (IL27) group (Figures 3C, 3D, 3F, and 3G)

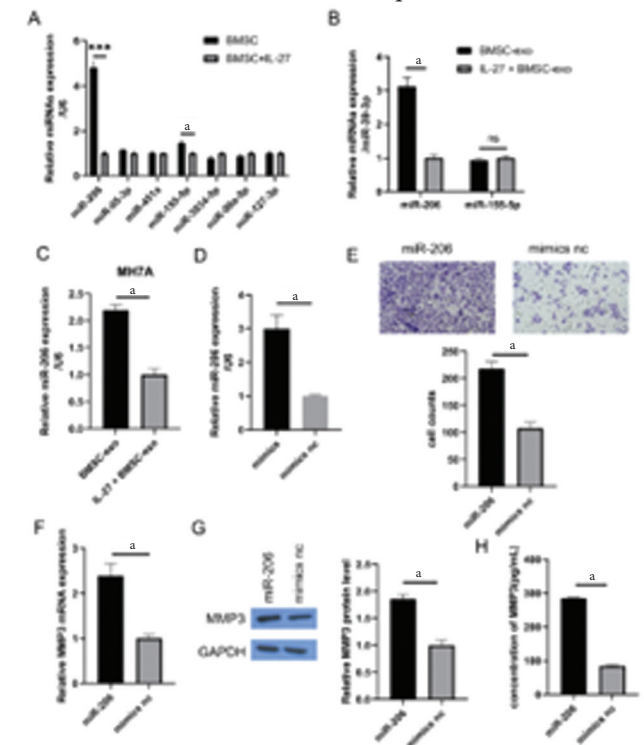
Abbreviations: ELISA, enzyme-linked immunosorbent assay; IL-27, interleukin-27; matrix metalloproteinase 3 (MMP3); MSC, mesenchymal stem cells; qRT-PCR, quantitative reverse transcription-polymerase chain reaction; WB, Western blot.

group ($P < .001$). Figure 4B shows that the BMSC-exo group's relative miR-206 was significantly higher than that of the IL-27+ BMSC-exo group. ($P < .001$)

Figure 4C shows that the BMSC-exo group's relative miR-206 expression was significantly higher than that of the IL-27+BMSC-exo ($P < .001$). Figures 4D shows that the mimics group's relative expression of miR-206 was significantly higher than that of the mimics nc group ($P < .001$).

High expression of miR-206 promoted the invasion of FLS (Figure 4E) and MMP3 expression and secretion of FLS

Figure 4. High Expression of miR-206 in IL-27-induced, MSC-derived exosomes, Promoting the Expression of MMP3 in FLS. Figure 4A shows the arthritis-related microRNAs in IL-27-induced MSC cells, detected using RT-qPCR; Figure 4B shows the arthritis-related microRNAs in IL-27-induced MSC exosomes, detected using RT-qPCR; Figure 4C shows the expression of miR-206 in exosome-treated MH7A cells, detected using qRT-PCR; Figure 4D shows the miR-206 mimics transfected into FLS MH7A cells and the transfection efficiency, detected using qPCR; Figure 4E shows the effect of miR-206 on the invasion of synovial fibroblast MH7A cells, detected using Transwell assays; and Figure 4F, 4G, and 4H show the effect of miR-206 on the expression and secretion of MMP3 in MH7A cells, detected qPCR, WB, and ELISA.

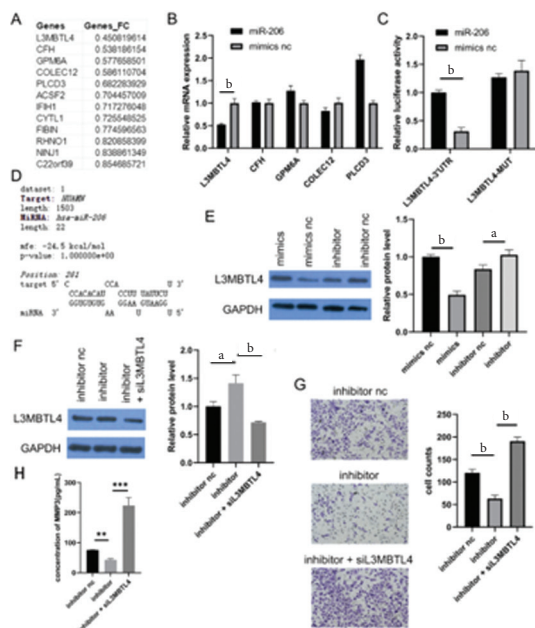


^a $P < .001$, indicating that the BMSC group's relative miR-206 and miR-155-5P expressions were significantly higher than those of the BMSC+IL-27 group (Figure 1A), that the BMSC-exo group's relative miR-206 was significantly higher than that of the IL-27+ BMSC-exo group (Figure 4B), that the BMSC-exo group's relative miR-206 expression was significantly higher than that of the IL-27+BMSC-exo (Figure 4C), that the mimics group's relative expression of miR-206 was significantly higher than that of the mimics nc group (Figure 4D), and that the miR-206 group's relative MMP3 mRNA expression, relative MMP3 protein levels, and concentration of MMP3 were significantly higher than those of the mimics nc group

Abbreviations: ELISA, enzyme-linked immunosorbent assay; FLS, fibroblast-like synoviocytes; IL-27, interleukin-27; matrix metalloproteinase 3 (MMP3); MSC, mesenchymal stem cells; qPCR, quantitative polymerase chain reaction; qRT-PCR, quantitative reverse transcription-polymerase chain reaction; WB, Western blot

(Figures 4F, 4G, and 4H). The miR-206 group's relative MMP3 mRNA expression, relative MMP3 protein levels, and concentration of MMP3 were significantly higher than those of the mimics nc group (all $P < .001$).

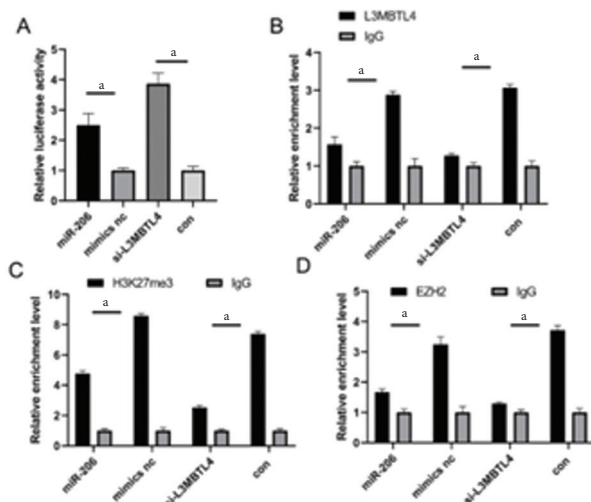
Figure 5. Promotion of the Transcription of MMP3 in FLS by miR-206 target microRNA-206 and lethal(3) malignant brain-tumor-like protein 4 (L3MBTL4). Figure 5A shows the Genetic Transformations of Candidate Targets of miR-206 in sequenced samples of arthritis and controls(Data from ArrayExpress E-MTAB-7313); Figure 5B shows the effect of miR-206 on candidate target genes, detected using RT-qPCR; Figure 5C shows the verification that miR-206 affects the 3' UTR of target genes, detected using dual luciferase assay; Figure 5D shows the BIBIServe software that predicted the site of the miR-206 target L3MBTL4; Figure 5E shows the inhibitory effect of miR-206 on L3MBTL4, verified using WB; Figure 5F shows the effect of the miR-206 inhibitor and L3MBTL4 knockdown on L3MBTL4 protein expression, detected using WB; Figure 5G shows the reverse experiment's verification that miR-206 regulates the migration and invasion of FLS MH7A cells by regulating L3MBTL4; and Figure 5H shows the effects of miR-206 on the expression and secretion of MH7A MMP3 in FLS by regulating L3MBTL4, detected using ELISA.



^a*P* < .05, indicating that the inhibitor nc group's relative protein level was significantly lower than that of the inhibitor group (Figure 5E), that the inhibitor nc group's relative protein level was significantly lower than that of the inhibitor group (Figure 5F), that the inhibitor nc group's concentration of MMP3 was significantly higher than that of the inhibitor group (Figure 5H) ^b*P* < .001, indicating that the miR-206 group's expression of L3MBTL4 was significantly lower than that of the mimics nc group (Figure 5B), that the miR-206 group's expression of L3MBTL4-3'UTR was significantly higher than that of the mimics nc group (Figure 5C), that the mimics nc group's relative protein level was significantly higher than that of the mimics nc group (Figure 5E), that the inhibitor + siL3MBTL4 group's relative protein level was significantly higher than that of the inhibitor group (Figure 5F), that the inhibitor nc group's cell count was significantly higher than that of the inhibitor group, and that the inhibitor + siL3MBTL4 group's cell count (Figure 5G) and concentration of MMP3 (Figure 5H) were significantly higher than that of the inhibitor group

Abbreviations: ELISA, enzyme-linked immunosorbent assay; FLS, fibroblast-like synoviocytes; matrix metalloproteinase 3 (MMP3); L3MBTL4, lethal (3) malignant brain tumor-like protein 4; miR-206, microRNA 206; qRT-PCR, quantitative reverse transcription-polymerase chain reaction; UTR, untranslated region; WB, Western blot.

Figure 6. L3MBTL4 regulated MMP3 transcription by regulating histone methylation in the promoter region. Figure 6A shows the effect of miR-206 and L3MBTL4 on the MMP3 promoter, detected using the Luciferase assay; Figure 6B shows the effect of miR-206 on L3MBTL4 and the effect of occupancy of the MMP3 promoter region, detected using ChIP-qRT-PCR; Figure 6C shows the effect of miR-206 and L3MBTL4 on the trimethylation of H3 histone Lys27 in the MMP3 promoter region, detected using ChIP-qRT-PCR; and Figure 6D shows the effects of miR-206 and L3MBTL4 on the occupancy of EZH2 in the promoter region of MMP3, detected using ChIP-qRT-PCR.



^a*P* < .001, indicating that the miR-206 group's relative luciferase activity was significantly higher than that of the mimics nc group and that the si-L3MBTL4 group's relative luciferase activity was significantly higher than that of the controls (Figure 6A), that the miR-206 group's relative enrichment level for L3MBTL4 was significantly lower than that of the mimics nc group and that the si-L3MBTL4 group's relative enrichment level for L3MBTL4 was significantly lower than that of the controls (Figure 6B), that the miR-206 group's relative enrichment level for H3K27me3 was significantly lower than that of the mimics nc group and that the si-L3MBTL4 group's relative enrichment level for H3K27me3 was significantly lower than that of the controls (Figure 6C), and that miR-206 group's relative enrichment level for EZH2 was significantly lower than that of the mimics nc group and that the si-L3MBTL4 group's relative enrichment level for EZH2 was significantly lower than that of the controls

Abbreviations: ChIP, chromatin immunoprecipitation; L3MBTL4, lethal (3) malignant brain tumor-like protein 4; matrix metalloproteinase 3; miR-206, microRNA 206; qRT-PCR, quantitative reverse transcription-polymerase chain reaction.

miR-206 target L3MBTL4

We refer to de Almeida R et al. who analyzed the expression network of RA-associated miRNAs related targets²⁹ and identified the top 5 genes with significant expression changes by qRT-PCR. Figure 5A shows the results of the target analysis of miR-206 in RA. Figure 5B shows that the miR-206 group's expression of L3MBTL4 was significantly lower than that of the mimics nc group (*P* < .001).

The dual luciferase analysis showed that miR-206 binds to the 3'UTR of L3MBTL4, and the BIBIServe software predicted the site of miR-206 targeting L3MBTL4 (Figures 5C and 5D). The miR-206 group's expression of L3MBTL4-3'UTR was significantly higher than that of the mimics nc group (*P* < .001).

The WB further confirmed that the miR-206 targeted L3MBTL4 (Figure 5E). The mimics nc group's relative protein level was significantly higher than that of the mimics group ($P < .001$). The inhibitor nc group's relative protein level was significantly lower than that of the inhibitor group ($P < .05$).

In silencing L3MBTL4 under miR-206-inhibited conditions to detect the effect of miR-206-L3MBTL4 interactions on FLS cell function, the WB showed that miR-206 effectively silenced L3MBTL4 (Figure 5F). The inhibitor nc group's relative protein level was significantly lower than that of the inhibitor group ($P < .05$) and the inhibitor + siL3MBTL4 group's relative protein level was significantly higher than that of the inhibitor group ($P < .001$).

The silencing of L3MBTL4 reversed the inhibitory effect of miR-206 inhibition on FLS invasion and secretion of MMP3 (Figures 5G and 5H). The inhibitor nc group's cell count ($P < .001$) and concentration of MMP3 ($P < .05$) were significantly higher than those of the inhibitor group, and the inhibitor + siL3MBTL4 group's cell count ($P < .001$) and concentration of MMP3 ($P < .001$) were significantly higher than that of the inhibitor group.

L3MBTL4-regulated MMP3 Transcription

The luciferase assay showed that both miR-206 upregulation and L3MBTL4 downregulation significantly promoted the transcriptional activity of the MMP3 promoter (Figure 6A). The miR-206 group's relative luciferase activity was significantly higher than that of the mimics nc group ($P < .001$), and the si-L3MBTL4 group's relative luciferase activity was significantly higher than that of the controls ($P < .001$).

The ChIP analysis of L3MBTL4 showed that miR-206 upregulation and L3MBTL4 downregulation attenuated L3MBTL4 localization to the MMP3 promoter region (Figure 6B). The miR-206 group's relative enrichment level for L3MBTL4 was significantly lower than that of the mimics nc group ($P < .001$), and the si-L3MBTL4 group's relative enrichment level for L3MBTL4 was significantly lower than that of the controls ($P < .001$).

The ChIP analysis of H3K27me3 showed that the upregulation of miR-206 and the downregulation of L3MBTL4 significantly downregulated the methylation of lysine 3 at position 27 of the H3 histone in the MMP3 promoter region (Figure 6C). The miR-206 group's relative enrichment level for H3K27me3 was significantly lower than that of the mimics nc group ($p < .001$), and the si-L3MBTL4 group's relative enrichment level for H3K27me3 was significantly lower than that of the controls ($P < .001$).

The ChIP analysis of EZH2 also confirmed that miR-206 upregulation and L3MBTL4 downregulation significantly reduced the EZH2 occupancy at the MMP3 promoter (Figure 6D). The miR-206 group's relative enrichment level for EZH2 was significantly lower than that of the mimics nc group ($P < .001$), and the si-L3MBTL4 group's relative enrichment level for EZH2 was significantly lower than that of the controls ($P < .001$).

Therefore, L3MBTL4 can regulate MMP3 transcription through PRC2 regulating histone methylation in the promoter region of MMP3.

DISCUSSION

In the present study, miR-206 targeted L3MBTL4 to activate MMP3 transcription in FLS. The study found that with the downregulation of L3MBTL4 in the MMP3 promoter region, the occupancy of the core protein EZH2 of PRC2 and the degree of trimethylation of the H3 histone Lys27 significantly decreased. This suggests that L3MBTL4 may recruit the PRC2 complex to inhibit the trimethylation of the three Lys27 histones, thereby inhibiting the transcription of MMP3.

CONCLUSIONS

IL-27 can induce the expression of miR-206 in MSCs, and miR-206 can be transported into FLS through MSC-EVs to promote FLS migration and MMP3 expression and aggravate articular cartilage damage. Patients with RA who have a high IL-27 expression may not be suitable to receive treatment with MSCs, and clinicians can use MSCs that knock down or delete IL-27R to treat RA patients who have a high IL-27 expression.

AUTHOR CONTRIBUTIONS

Ma Lihui and Liu Yueli contributed equally to the work.

AUTHORS' DISCLOSURE STATEMENT

The Hainan Provincial Natural Science Foundation of China (No:2019RC378) supported the research. The authors declare that they have no conflicts of interest related to the study.

REFERENCES

- Di D, Zhang L, Wu X, Leng R. Long-term exposure to outdoor air pollution and the risk of development of rheumatoid arthritis: A systematic review and meta-analysis. *Semin Arthritis Rheum*. 2020;50(2):266-275. doi:10.1016/j.semarthrit.2019.10.005
- Castor CW. The microscopic structure of normal human synovial tissue. *Arthritis Rheum*. 1960;3(2):140-151. doi:10.1002/art.1780030205
- Cross M, Smith E, Hoy D, et al. The global burden of rheumatoid arthritis: estimates from the global burden of disease 2010 study. *Ann Rheum Dis*. 2014;73(7):1316-1322. doi:10.1136/annrheumdis-2013-204627
- Myasoedova E, Davis J, Matteson EL, Crowson CS. Is the epidemiology of rheumatoid arthritis changing? Results from a population-based incidence study, 1985-2014. *Ann Rheum Dis*. 2020;79(4):440-444. doi:10.1136/annrheumdis-2019-216694
- Smolen JS, Aletaha D, McInnes IB. Rheumatoid arthritis. *Lancet*. 2016;388(10055):2023-2038. doi:10.1016/S0140-6736(16)30173-8
- McInnes IB, Schett G. The pathogenesis of rheumatoid arthritis. *N Engl J Med*. 2011;365(23):2205-2219. doi:10.1056/NEJMra1004965
- Mahmoud DE, Kaabachi W, Sassi N, et al. The synovial fluid fibroblast-like synoviocyte: A long-neglected piece in the puzzle of rheumatoid arthritis pathogenesis. *Front Immunol*. 2022;13:942417. doi:10.3389/fimmu.2022.942417
- Guerrero S, Sánchez-Tirado E, Agüí L, González-Cortés A, Yáñez-Sedeño P, Pingarrón JM. Simultaneous determination of CXCL7 chemokine and MMP3 metalloproteinase as biomarkers for rheumatoid arthritis. *Talanta*. 2021;234:122705. doi:10.1016/j.talanta.2021.122705
- Lerner A, Neidhöfer S, Reuter S, Matthias T. MMP3 is a reliable marker for disease activity, radiological monitoring, disease outcome predictability, and therapeutic response in rheumatoid arthritis. *Best Pract Res Clin Rheumatol*. 2018;32(4):550-562. doi:10.1016/j.berh.2019.01.006
- Zhang C, Chen L, Gu Y. Polymorphisms of MMP-1 and MMP-3 and susceptibility to rheumatoid arthritis: A meta-analysis. *Z Rheumatol*. 2015;74(3):258-262. doi:10.1007/s00393-014-1537-2
- Audo R, Deckert V, Daien CI, et al. Phospholipid transfer protein (PLTP) exerts a direct pro-inflammatory effect on rheumatoid arthritis (RA) fibroblasts-like-synoviocytes (FLS) independently of its lipid transfer activity. *PLoS One*. 2018;13(3):e0193815. doi:10.1371/journal.pone.0193815
- Liu H, Li R, Liu T, Yang L, Yin G, Xie Q. Immunomodulatory Effects of Mesenchymal Stem Cells and Mesenchymal Stem Cell-Derived Extracellular Vesicles in Rheumatoid Arthritis. *Front Immunol*. 2020;11:1912. doi:10.3389/fimmu.2020.01912
- Gowhari Shabgah A, Shariati-Sarabi Z, Tavakkol-Afshari J, Ghasemi A, Ghoryani M, Mohammadi M. A significant decrease of BAFF, APRIL, and BAFF receptors following mesenchymal stem cell transplantation in patients with refractory rheumatoid arthritis. *Gene*. 2020;732:144336. doi:10.1016/j.gene.2020.144336
- Yu Y, Yoon KA, Kang TW, et al. Therapeutic effect of long-interval repeated intravenous administration of human umbilical cord blood-derived mesenchymal stem cells in DBA/1 mice with collagen-induced arthritis. *J Tissue Eng Regen Med*. 2019;13(7):1134-1142. doi:10.1002/term.2861
- Spees JL, Lee RH, Gregory CA. Mechanisms of mesenchymal stem/stromal cell function. *Stem Cell Res Ther*. 2016;7(1):125. doi:10.1186/s13287-016-0363-7
- Kodama J, Wilkinson KJ, Otsuru S. MSC-EV therapy for bone/cartilage diseases. *Bone Rep*. 2022;17:101636. doi:10.1016/j.bonr.2022.101636

17. Buckley CD, Ospelt C, Gay S, Midwood KS. Location, location, location: how the tissue microenvironment affects inflammation in RA. *Nat Rev Rheumatol*. 2021;17(4):195-212. doi:10.1038/s41584-020-00570-2
18. Millier MJ, Lazaro K, Stamp LK, Hessian PA. The contribution from interleukin-27 towards rheumatoid inflammation: insights from gene expression. *Genes Immun*. 2020;21(4):249-259. doi:10.1038/s41435-020-0102-z
19. Lalive PH, Kreutzfeldt M, Devergne O, et al. Increased interleukin-27 cytokine expression in the central nervous system of multiple sclerosis patients. *J Neuroinflammation*. 2017;14(1):144. doi:10.1186/s12974-017-0919-1
20. Lai X, Wang H, Cao J, et al. Circulating IL-27 Is Elevated in Rheumatoid Arthritis Patients. *Molecules*. 2016;21(11):1565. doi:10.3390/molecules21111565
21. Hou J, Gao W. IL-27 regulates autophagy in rheumatoid arthritis fibroblast-like synoviocytes via STAT3 signaling. *Immunobiology*. 2022;227(4):152241. doi:10.1016/j.imbio.2022.152241
22. Wong CK, Chen DP, Tam LS, Li EK, Yin YB, Lam CW. Effects of inflammatory cytokine IL-27 on the activation of fibroblast-like synoviocytes in rheumatoid arthritis. *Arthritis Res Ther*. 2010;12(4):R129. doi:10.1186/ar3067
23. Han L, Chen Z, Yu K, et al. Interleukin 27 Signaling in Rheumatoid Arthritis Patients: good or Evil? *Front Immunol*. 2022;12:787252. doi:10.3389/fimmu.2021.787252
24. Xu F, Yi J, Wang Z, et al. IL-27 regulates the adherence, proliferation, and migration of MSCs and enhances their regulatory effects on Th1 and Th2 subset generations. *Immunol Res*. 2017;65(4):903-912. doi:10.1007/s12026-017-8929-8
25. Chen Z, Wang H, Xia Y, Yan F, Lu Y. Therapeutic Potential of Mesenchymal Cell-Derived miRNA-150-5p-Expressing Exosomes in Rheumatoid Arthritis Mediated by the Modulation of MMP14 and VEGF. *J Immunol*. 2018;201(8):2472-2482. doi:10.4049/jimmunol.1800304
26. Zheng J, Zhu L, Iok In I, Chen Y, Jia N, Zhu W. Bone marrow-derived mesenchymal stem cells-secreted exosomal microRNA-192-5p delays inflammatory response in rheumatoid arthritis. *Int Immunopharmacol*. 2020;78:105985. doi:10.1016/j.intimp.2019.105985
27. Meng HY, Chen LQ, Chen LH. The inhibition by human MSCs-derived miRNA-124a overexpression exosomes in the proliferation and migration of rheumatoid arthritis-related fibroblast-like synoviocyte cell. *BMC Musculoskelet Disord*. 2020;21(1):150. doi:10.1186/s12891-020-3159-y
28. Debreova M, Culenova M, Smolinska V, Nicodemou A, Csobonyeiova M, Danisovic L. Rheumatoid arthritis: from synovium biology to cell-based therapy. *Cytotherapy*. 2022;24(4):365-375. doi:10.1016/j.jcyt.2021.10.003
29. Coutinho de Almeida R, Ramos YFM, Mahfouz A, et al. RNA sequencing data integration reveals an miRNA interactome of osteoarthritis cartilage. *Ann Rheum Dis*. 2019;78(2):270-277. doi:10.1136/annrheumdis-2018-213882